International Journal of Life science & Pharma Research

IN-SILICO STUDY OF HERBAL COMPOUNDS (BAICALIN, CURCUMIN AND DRONABINOL) AS NOVEL MAO INHIBITORS FOR PARKINSON'S DISEASE TREATMENT

RAKSHA SINGH[1], NAVNEET CHATURVEDI[2] AND VINAY KUMAR SINGH[1]*

[1]Centre for Bioinformatics, School of Biotechnology, Faculty of Science, Banaras Hindu University, Varanasi-221005, INDIA
[2]Center of Bioinformatics, University of Allahabad, Allahabad, INDIA

ABSTRACT

Parkinson disease (PD) is the second most common neurodegenerative disorder. MAO A and MAO B have important functions in the metabolism of neuroactive and vasoactive amines in the central nervous system. Monoamine oxidase inhibitors may limit the rate of dyskinesia relative to levodopa, the standard therapy for motor control of PD. The MAOs site represents a central target for therapeutics of Parkinson's disease and major depressive disorder. Monoamine Oxidase (MAOs) isoforms have amine oxidase domain (IPR001613, IPR002937), we have taken the functional signature part to study their homologues in human genome and successfully hunted 14 isoforms related to this family. Templates were selected with 99% sequence identity for both Mao A and Mao B isoforms. 3D structure of MAO A and MAO B were generated, evaluated and submitted to PMDB database and are available with PMDBID; PM0077964, PM0077935 respectively. Some novel herbal bioactive compounds (Baicalin, Curcumin and Dronabinol) have been reported to be useful in neurodegerative disorders, depression and have antioxidative property. Docking was successfully performed for MAO A and MAO B proteins with Baicalin, Curcumin and Dronabinol bioactive compounds and active site coordination was found to be similar as the template residues involved in binding with experimentally used inhibitors. The residues which are involved in the hydrophobic, cation-pi, pi-pi interaction and hydrogen bonding etc. also representing the similarity with the predicted active sites-1 by using Q-site finder with major interacting surface area. Among these three compounds, most effective compound was found to be Dronabinol as showing minimum Inhibition Constant, Ki and lowest free energy of binding for both models. This knowledge may be important for the development of novel drugs for the treatment of Parkinson disease and other neurodegenrative disorders.

Keywords: Neurodegeneration, Parkinson disease, modeling, Monoamine oxidase inhibitors, docking.

INTRODUCTION

Parkinson's disease (PD) is a degenerative disorder of the central nervous system. Parkinson's disease belongs to a group of conditions called movement disorders. MAO A and MAO B play important role in the metabolism of neuroactive and vasoactive amines in the central nervous system [Shih JC et al., 1999]. Monoamine oxidase inhibitors (MAOIs) block the degradation of the monoamine neurotransmitters inhibiting the enzyme monoamine oxidase, leading to increased concentrations of these neurotransmitters in the

brain and an increase in neurotransmission reduce the symptoms of PD [Kleinman A. et al.,2006].
In this work, a molecular docking technique was used to envisage the binding orientation of small molecules to their protein targets to predict the affinity and activity of the drug. Docking plays important role in the rational drug design and development of the vaccines. The modern bioinformatics programs/softwares i.e. Q-site finder, Docking server, and Discovery studio have been used to find the active sites of the MAO proteins. The structure of ligand against the active binding site can be found by Molecular Docking Server and DS Vizualizer. The exact conformation and configuration of the ligand can be calculated to find the best molecule with minimum binding energy and it can be used to develop potential drug molecule against the disease. Some herbal bioactive compounds have been reported to be useful in neurodegerative disorders. In this case herbal compounds block MAO's active sites and can be used as novel potent drugs for the treatment of Parkinson disease.

MATERIALS AND METHODS

Retrieval of amine oxidase proteins and chromosomal localization prediction

The amino acid sequence of monoamine oxidase with accession number NP_000231.1 of *Homo sapiens* was retrieved from NCBI database and was used for homology search using Basic Local Alignment Search Tool [Altschul SF et al., 1990] against Homo sapiens neanderthalensis genome sequence from NCBI database. Protein functional elucidation was done on the basis of amine oxidase domain using Interproscan server (http: //www. ebi.ac.uk/ Tools/pfa/iprscan/). Mapping of all the isoforms was done and chromosomal localization was determined using Human genome BLAST.

Phylogenetic relationship and Physico-chemical properties

For multiple sequence analysis Clustalw tool (http://www.ebi.ac.uk/Tools/msa/clustalw2/) [Thompson JD et al., 2002] was used and phylogenetic tree was constructed based on NJ (Neighbor joining) plot. Prot Param was used to predict physiochemical properties. The parameters computed by Prot Param included the molecular weight, theoretical PI, aliphatic index and grand average of hydropathicity (GRAVY).

Homology modeling, Quality assessment and visualization

Homology modeling was used to determine the 3D structure of amine oxidase isoforms. A BLASTP search with default parameters was performed against the Brookhaven Protein Data Bank (PDB) to find suitable templates for homology modeling. Templates with PDB ID: 2z5yA , 2v5Za were identified on the basis of sequence identity (more than 99.8%) for MAO A and MAO B respectively. The Protein Structure Prediction Server Swiss model [Arnold K et al., 2006] (http://swissmodel.expasy.org/) was used for homology model construction. Once the 3D models of proteins were generated, structural evaluation and stereochemical analysis was performed using RAMPAGE (http://mordred.bioc.cam.ac.uk/~rapper/rampage.php). Z-score was also used to check the reliability of predicted 3D model. Z score of the generated model was determined by SWISS MODEL [Schwede T et al., 2003]. Errat server was used to find the accuracy of the model and visualization of generated models was performed using UCSF chimera 1.5.3 [Yang Z et al., 2011].

Active site prediction

Q-Site Finder server [Laurie AT et al., 2005] (www.modelling.leeds.ac.uk/qsitefinder/) was used to predict the ligand binding site. This server calculate the possible active sites from the 3D atomic coordinates of the protein model.PDB file was upload in server and it showed residues involved in ligand binding site, site volume and protein volume for ten active sites.

Ligand optimization and docking study

Reported inhibitory compounds were retrieved from PubChem Compound Database (http://www.ncbi.nlm.nih.gov/pccompound). Sdf files of Ligands were converted in PDB file using Discovery studio vizualizer and geometry was cleaned by clean geometry menu of Discovery

studio 3.0 and saved for further computational analysis. These PDB ligand files and MAO and MAO B were imported to Molecular docking server for docking. Docking server was used to calculate molecular weight, molecular formula, molar weight and MMFF94 energy calculation of all retrieved compounds. Molecular Docking Server was used for docking studies which is based on modeling force field and Gasteiger charge calculation method [Bikadi et al., 2009; Morris et al., 1998; Solis and Wets, 1981]. Docking results give different conformations of ligand from single 3D conformations by applying a collection of preferred torsion angles to the rotatable bonds.

RESULTS

Retrieval of amine oxidase domain containing proteins and chromosomal localization

Based on functional domain sequence of well characterized gene/protein, homology search was done using Basic Local Alignment Search Tool (BLAST) against Homo sapiens neanderthalensis genome sequence from NCBI database. We have successfully hunted 14 isoforms [Table 1]. Interproscan study revealed that all homologues proteins were belonging to IPR001613 (Flavin amine oxidase), IPR002937 (Amine oxidase) family [Fig.1]. These isoforms belong to Polyamine Oxidase (PAO), Monoamine Oxidase (MAO), L-amino acid oxidase (LAO), Protoporphyrinogen Oxidase (PPOX), Lysine Specific Histone Demethylase (LSHD) and Spermine Oxidase (SOX) genes of amine oxidase gene family. MAO isoforms were located on X chromosome, LAO on 19 chromosome, LSHD on 1 and 6 chromosome. Locus of PAO was found to be on 10 chromosome, PPOX on 1 and SOX isoforms were present on 10 and 20 chromosome [Fig. 2].

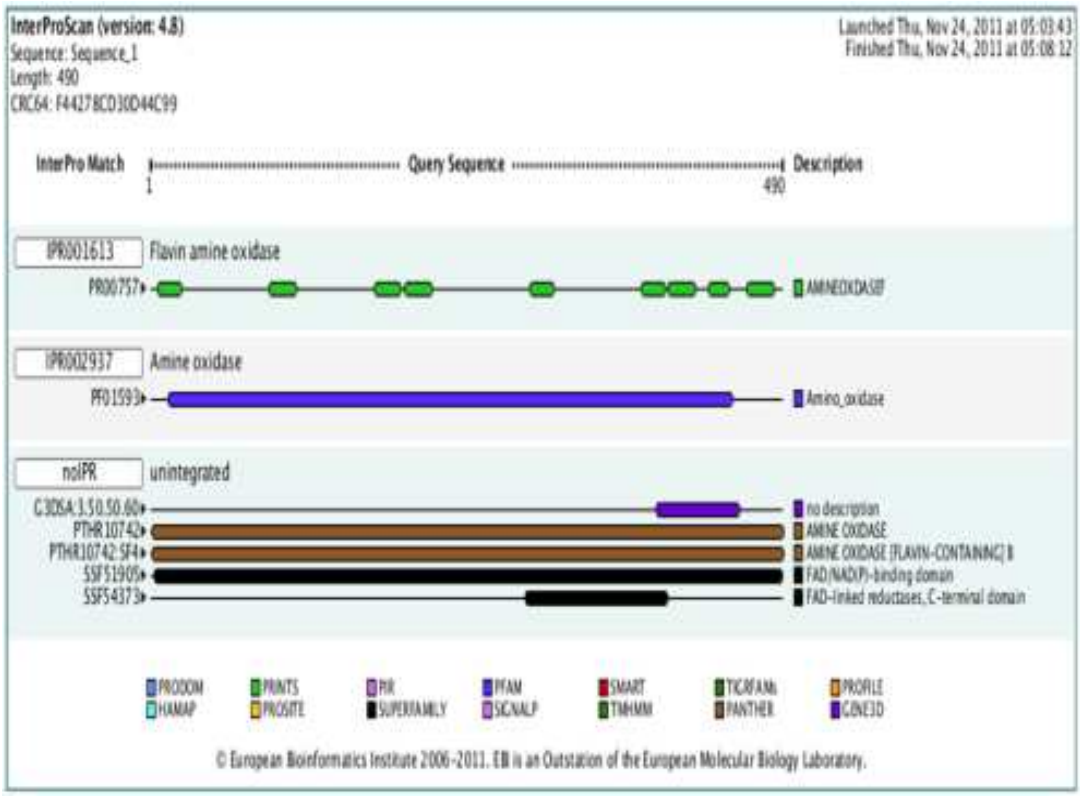

Figure 1: ***Interproscan Result for protein domain identification***

Table 1: ***Hunted amine oxidase domain containing proteins***

Sr. No	Accession	Protein	NCBI Ref Sequence	Start	End	Chr.
1	NP_000889.3	amine oxidase [flavin-containing] B	NW_001842361.2	1380579	1467657	X
2	NP_000231.1	amine oxidase [flavin-containing] A	NW_001842361.2	1380579	1467657	X
3	NP_758962.1	L-amino-acid oxidase isoform 2	NT_011109.16	22661145	22673192	19
4	NP_690863.1	L-amino-acid oxidase isoform 1	NT_011109.16	22661145	22667635	19
5	NP_055828.2	lysine-specific histone demethylase 1A isoform b	NW_001838573.1	4965991	5030449	1
6	NP_001009999.1	lysine-specific histone demethylase 1A isoform a	NW_001838573.1	4965991	5030449	1
7	NP_694587.3	lysine-specific histone demethylase 1B	NT_007592.15	18100127	18162223	6
8	NP_690875.1	polyamine oxidase isoform 1	NT_008818.16	6426752	6438890	10
9	NP_997011.1	polyamine oxidase isoform 4	NT_008818.16	6426752	6438890	10
10	NP_000300.1	protoporphyrinogen oxidase	NT_004487.19	12625280	12629608	1
11	NP_787033.1	spermine oxidase isoform 1	NW_001838014.1	1775828	1787960	10
12	NP_787034.1	spermine oxidase isoform 2	NW_001838014.1	1775828	1785574	10
13	NP_787035.1	spermine oxidase isoform 3	NT_011387.8	4129450	4168369	20
14	>NP_787036.1	spermine oxidase isoform 4	NT_011387.8	4095703	4108054	20

Figure 2: ***Mapping of identified gene members in human genome***

Phylogenetic relationship and Physico-chemical properties

For multiple sequence analysis ClustalW tool was used and found that amino acid residues were conserved in most of the isoforms [Fig. 3]. Phylogenetic study revealed that PPOX was differ from others and MAO, LAO were in same cluster as share more homology while LSHD, SOX and PAO in another cluster [Fig.4]. ProtParam showed that Mol. wt. of MAO A and MAO B was 59681.6 and 58762.8 Daltons respectively [Table 2]. An isoelectric point was 7.94 and 7.20 for MAO A and MAO B which indicates positively charged proteins. The negative GRAVY index of -0.279 and -0.236 is indicative of hydrophilic and soluble proteins.

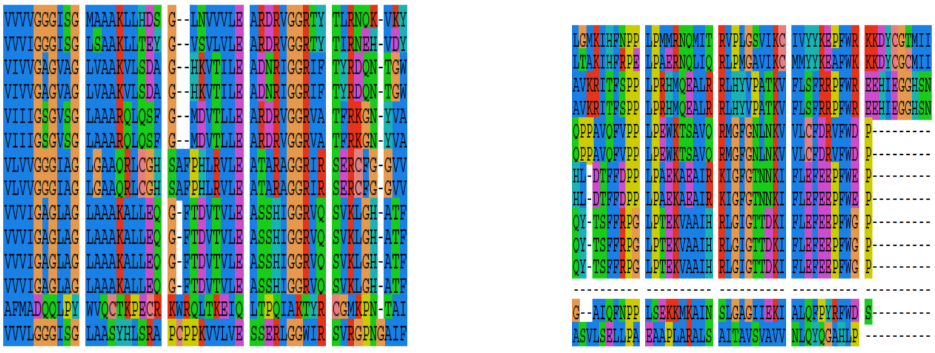

Figure 3: ***Multiple Sequence Alignment (MSA) of all amine oxidase isoforms.***

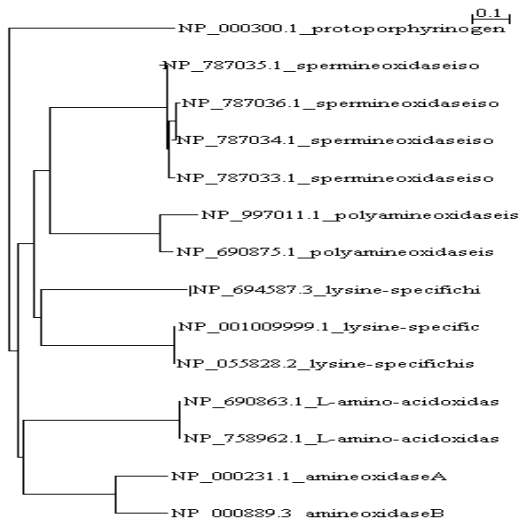

Figure 4: ***Tree generation using NJ plot***

Table 2: ***Physico-chemical properties of hunted genes***

S.N.	Gene Name	Molecular weight	Theoretical PI	Aliphatic index	Grand average of hydropathicity (GRAVY)
1.	NP_000889.3_amineoxidaseB	58762.8	7.20	88.85	-0.236
2.	NP_000231.1_amineoxidaseA	59681.6	7.94	86.19	-0.279
3.	NP_758962.1_L-amino-acidoxidaseisoform2	65327.7	8.69	87.78	-0.306
4.	NP_690863.1_L-amino-acidoxidaseisoform1	62881.0	8.79	90.32	-0.274
5.	NP_055828.2_lysine-specifichistonedemethylase1A	92902.6	6.11	81.44	-0.371
6.	NP_001009999.1_lysine-specifichistonedemethylase1A	95154.8	5.90	80.22	-0.388
7.	NP_694587.3_lysine-specifichistonedemethylase1B	65717.1	8.80	73.25	-0.382
8.	NP_690875.1_polyamineoxidaseisoform1	55513.0	5.12	88.18	-0.013
9.	NP_997011.1_polyamineoxidaseisoform4	51963.1	4.94	88.29	0.079
10.	NP_000300.1_protoporphyrinogenoxidase	50765.3	8.43	100.42	0.041
11.	NP_787033.1_spermineoxidaseisoform1	61819.2	5.29	75.71	-0.468
12.	NP_787034.1_spermineoxidaseisoform2	56091.1	5.83	76.93	-0.428
13.	NP_787035.1_spermineoxidaseisoform3	20630.0	6.23	82.68	-0.341
14.	NP_787036.1_spermineoxidaseisoform4	59278.7	6.05	74.98	-0.466

Homology modeling

Protein 3D structure prediction can provide us precise functional information of how proteins interact and localize in their stable conformation. Homology or comparative modeling is one of the most common structure prediction methods in structural genomics and proteomics. Numerous online servers and tools have become available for homology or comparative modeling of proteins. The best matching templates were selected for both target protein on the basis of sequence homology using PDB Advance Blast. Templates are experimentally determined 3D structure of proteins that share sequence similarity with target sequence. A well-defined alignment is very important for the reliable prediction of a 3D structure. The template sequence and the target protein sequence were aligned using BLASTP alignment tool. Templates

showed sequence identity greater than 99.8% for both MAO A and MAO B isoforms. 3D structure of MAO A and MAO B were generated using Swiss Model Server [Arnold K et al., 2006] [Fig. 5 and Fig. 7]. The Z-score is indicative of overall model quality and is used to check whether the input structure is within the range of scores typically found for native proteins of similar size. Z score of the template and query model was obtained by SWISS MODEL. Z score for MAO A and MAO B was 0.382, 0.614, suggesting a good structure [Table 3].

Table 3:*Swiss Model server result showing the template structure used in homology modeling, Sequence identity, quality score and ligand associated with templates*

Sr. No.	Gene Name	Modelled residue range	Based on template	Resolution (Å)	Sequence Identity	QMEAN Z-Score	Ligands in the template
1	**MAOA**	12 - 524	2z5yA	2.17	99.805%	-0.614	DCX: 2, FAD:1, HRM: 1.
2	**MAOB**	3 -501	2v5zA	1.6	100 %	-0.382	FAD:2 SAG:2

Quality assessment and visualization

3D structure of MAO A and MAO B were generated. Even though there were no stearic clashes in the structure generated, both models were assessed for geometric and energy aspects. Ramachandran plot was used to check the reliability of predicted 3D model. RAMPAGE (http://mordred.bioc.cam.ac.uk/~rapper/rampage.php) checks the stereochemical quality of a protein structure by analyzing residue-by-residue geometry and overall structure geometry. Ramachandran plots were obtained for both MAO models for quality assessment. RAMPAGE displayed 97.8% of residues in the most favoured regions, 2.2% residues in additionally allowed and 0.0% disallowed regions for MAO A model and in case of MAO B model, 96.5% of residues in the most favoured regions, 3.5% residues in additionally allowed and no residues in disallowed regions [Fig. 6 and Fig. 8]. Errat (http://nihserver.mbi.ucla.edu/ERRATv2/) Server was used to find the accuracy of the model. Result of Errat showed 97.426% accurate structure for MAO A and 80.354 for MAO B. The final protein structures of both MAO isoforms were submitted to the protein Model Database (PMDB) (http://mi.caspur.it/PMDB/) and are available with PMDB ID: PM0077964 and PM0077935.

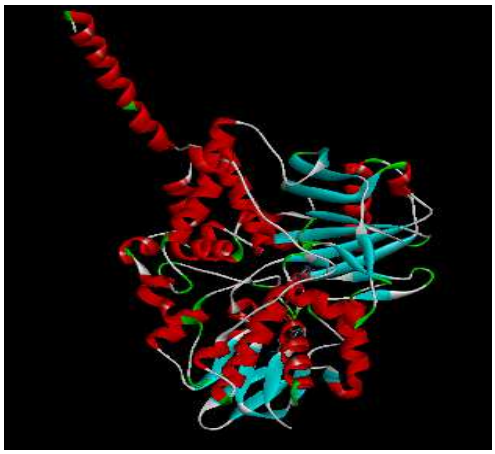

Figure 5: ***MAO B 3D model***

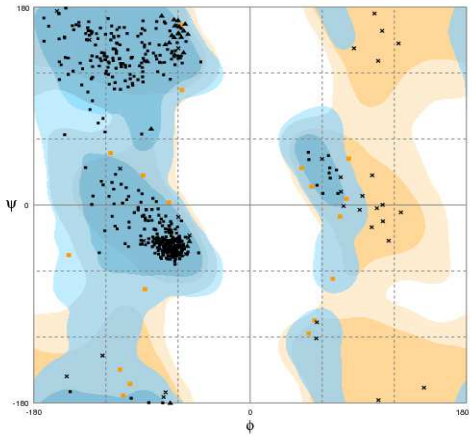

Figure 6: ***MAO B RAMPAGE result***

Figure 7: ***MAO A 3D model***

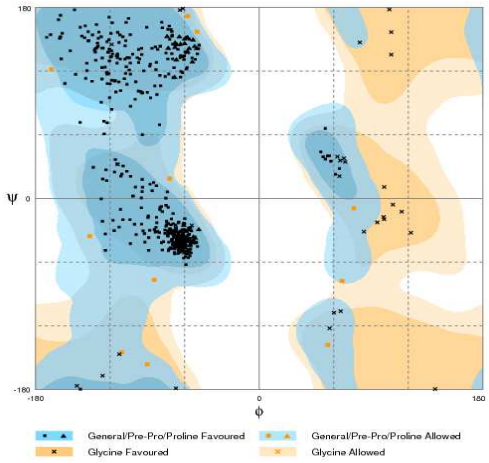

Figure 8: ***MAO A RAMPAGE result***

Protein structure accession number

The predicted 3D structure of MAO A and MAO B were submitted to the protein Model Database (PMDB) and assigned the PMDB ID: PM0077964, PM0077935 respectively.

Active site identification

Q-SiteFinder server was used to predict the ligand binding site. This server calculates the possible active sites from the 3D atomic coordinates of the protein model. Active site prediction is useful to determine potential sites for ligand binding in molecular docking. Residues involved in ligand binding site, site volume and protein volume for ten active sites for both MAO A and MAO B were predicted. Among the ten binding sites obtained from Q-SiteFinder for MAO A [Table 5], site 1 was highly conserved within the active site of the template. The Predicted site 1 consisted 1357 Cubic angstroms site volume out of the 49534 Cubic Angstroms of protein volume. The residues in site 1 ILE^{19},GLY^{20},GLY^{21},GLY^{22},ILE^{23},SER^{24},GLY^{25},LEU^{42},GLU^{43}, ALA^{44}, ARG^{45}, GLY^{49},GLY^{50},ARG^{51},THR^{52},VAL^{65},GLY^{66},GLY^{67}, ALA^{68},TYR^{69},VAL^{70},GLN^{74},LEU^{97},PHE^{108},GLY^{110}, ALA^{111},ILE^{180},ASN^{181},VAL^{182},TYR^{197},ILE^{207},PHE^{208},SER^{209},VAL^{210},GLY^{214},GLN^{215},SER^{227},HIS^{242},PRO^{243},VAL^{244},THR^{245},ALA^{272},ILE^{273},PRO^{274},LEU^{277},THR^{278},LYS^{280},ILE^{281},VAL^{303},LYS^{305},CYS^{323},ILE^{325},ILE^{335},THR^{336},LEU^{337},MET^{350},PHE^{352},TRP^{397}, GLN^{401},TYR^{402},SER^{403},CYS^{406},TYR^{407},THR^{408},GLY^{434},THR^{435},GLU^{436},GLY^{443},TYR^{444}, MET^{445}, GLU^{446},and ALA^{448} are similar with the active site of the template .

Among the ten binding sites obtained from Q-Site Finder for MAO B [Table 4], site 1 was highly conserved within the active site of the template. The Predicted site 1 consisted 1085 Cubic angstroms site volume out of the 49420 Cubic Angstroms of protein volume. The residues in site 1, VAL^{10}, GLY^{11}, GLY^{12}, GLY^{13}, ILE^{14}, SER^{15}, GLY^{16}, LEU^{33},GLU^{34},ALA^{35},ARG^{36},ARG^{38}, VAL^{39}, GLY^{40},GLY^{41},ARG^{42}, THR^{43}, LEU^{56}, GLY^{57}, GLY^{58}, SER^{59}, TYR^{60}, VAL^{61}, GLN^{65}, PHE^{168}, LEU^{171}, CYS^{172}, TYR^{188}, ILE^{198}, ILE^{199}, GLY^{205}, GLN^{206}, SER^{218}, VAL^{235}, ALA^{263}, ILE^{264}, PRO^{265}, LEU^{268}, VAL^{294}, LYS^{296}, TYR^{326}, LEU^{328}, MET^{341}, PHE^{343}, TRP^{388}, TYR^{393}, SER^{394}, CYS^{397}, TYR^{398}, THR^{399}, GLY^{425}, THR^{426}, GLU^{427}, GLY^{434}, TYR^{435}, MET^{436}, GLU^{437}, and ALA^{439} are similar with the active site of the template . Thus, only site 1has been chosen in this study as the most favorable site for docking and the other sites are not further discussed.

Table 4: *MAO B active site*

Site	Residues involved in Ligands binding site	Site Volume (Cubic Angstroms)
Site 1 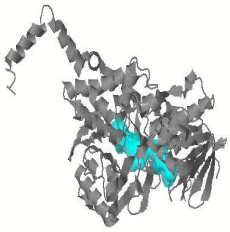	VAL[10],GLY[11],GLY[12],GLY[13],ILE[14],SER[15],GLY[16],LEU[33],GLU[34],ALA[35], ARG[36],ARG[38], VAL[39], GLY[40],GLY[41],ARG[42], THR[43], LEU[56], GLY[57], GLY[58] , SER[59], TYR[60], VAL[61], GLN [65], PHE[168], LEU[171], CYS[172], TYR[188], ILE[198], ILE[199], GLY[205], GLN [206], SER[218], VAL[235], ALA [263], ILE[264], PRO[265], LEU[268], VAL[294], LYS[296], TYR[326], LEU[328], MET[341], PHE[343], TRP[388], TYR[393], SER[394], CYS[397], TYR[398], THR[399], GLY[425], THR[426], GLU[427], GLY[434], TYR[435], MET[436], GLU[437], ALA[439]	1085
Site 2 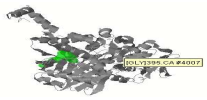	GLU[84], VAL[85], GLU[86], ARG[87], LEU[88], PHE[99], ARG[100], GLY[101], PRO[102], PHE[103], PRO[104], TRP [119], LEU[164], LEU[167], PHE[168], LEU[171], ILE[198], ILE[199], SER[200], THR[201],THR[202], ASN[203], GLN[206], THR[314], ILE[316], TYR[326]	473
Site3 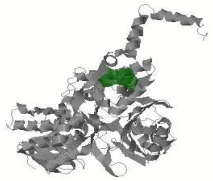	PHE[103], PRO[104], PRO[105], VAL[106], TYR[112], HIS[115], ASN[116], TRP[119],ARG[120], ASP[123], ARG[127], LEU[164], THR[195], THR[196], ILE[477], THR[478], THR[479], THR[480], LEU[482], GLU[483], ARG[484]	421
Site4 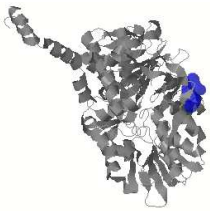	ASN[66], ILE[68], LEU[69], ARG[70], ALA[72], LYS[73], LEU [77], GLU[78], THR[79], ARG[208], PHE[210], GLU[466], PRO[467], GLU[468], SER[469], VAL[470],ASP[471], VAL[472]	332
Site5 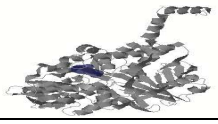	ARG[42], SER[131], ASP[132], ALA[133], PRO[134], TRP[135],TRP [184], TRP[187], TYR[188], THR[399], THR[400], TYR[401], PHE[402], LEU[407], GLY[411], LEU[414], ARG[415], THR[426], GLU[427], THR[428], ALA[429], THR[430], SER[433],GLY[434]	216
Site6 	HIS[90],VAL[92],LYS[93],TYR[97],PHE[99],PHE[103],PRO[104],PRO[105],VAL[106], TRP[107], ASN[108], THR[111], HIS[115], TRP[119], GLU[159], SER[160], ALA[161], GLN[163], LEU[164], ASP[318]	290
Site7	LYS [93], GLN [163], THR[166], LEU[167], ASN[170], ILE[317], ASP[318], GLY[319], GLU[320], ALA[325], LEU[345], ALA[346], HIS[347], LYS[348]	242

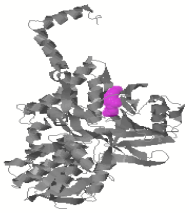		
Site8 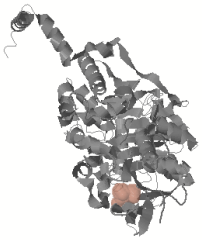	VAL^{10}, GLY^{11}, GLY^{12}, LEU^{33}, GLU^{34}, ALA^{35}, ARG^{233}, PRO^{234},VAL^{235}, ILE^{236}, ILE^{264}, LEU^{268}, GLY^{269}, LYS^{271}, ILE^{272}, GLN^{392} TYR^{393}	187
Site9 	ILE^{295}, CYS^{297}, PRO^{323}, ILE^{344}, LYS^{348}, ALA^{349}, LEU^{352}, ALA^{353}, ARG^{354}, LEU^{355}, THR^{356}, LYS^{357}, GLU^{359}, ARG^{360}, LEU^{364}, GLU^{385}, ASN^{387}, GLU^{390}	168
Site10	VAL^{51}, LYS^{52}, TYR^{53}, VAL^{54}, ASP^{55}, TYR^{80}, LYS^{209}, ILE^{298}, TYR^{300}, ASP^{330}, THR^{331}, LYS^{332}, PRO^{333}, ASN^{336}, TYR^{337}, ALA^{339}	133

Table 5: ***MAO A active site***

Site	Residues involved in Ligands binding site	Site Volume (Cubic Angstroms)
Site1 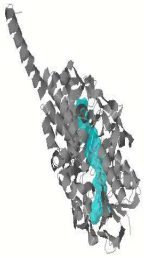	ILE^{19},GLY^{20},GLY^{21},GLY^{22},ILE^{23},SER^{24},GLY^{25},LEU^{42},GLU^{43},ALA^{44},ARG^{45},GLY^{49} ,GLY^{50},ARG^{51}, THR^{52},VAL^{65},GLY^{66},GLY^{67},ALA^{68},TYR^{69},VAL^{70},GLN^{74},LEU^{97},PHE^{108},GLY^{110},A LA^{111},ILE^{180},ASN^{181},VAL^{182},TYR^{197},ILE^{207},PHE^{208},SER^{209},VAL^{210},GLY^{214},GLN^{215}, SER^{227},HIS^{242},PRO^{243},VAL^{244}, THR^{245},ALA^{272},ILE^{273},PRO^{274},LEU^{277},THR^{278},LYS^{280},ILE^{281},VAL^{303},LYS^{305},CYS^{32} ^{3},ILE^{325},ILE^{335} THR^{336},LEU^{337},MET^{350},PHE^{352},TRP^{397},GLN^{401},TYR^{402},SER^{403},CYS^{406},TYR^{407},THR ^{408},GLY^{434},THR^{435},GLU^{436},GLY^{443},TYR^{444},MET^{445},GLU^{446},ALA^{448}	1357
Site2 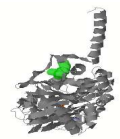	PHE^{112},PRO^{113},PRO^{114},VAL^{115},TYR^{121},TYR^{124},ASN^{125},TRP^{128},ARG^{129},ASP^{132},ASN ^{133},LYS^{136}, THR^{204},THR^{205},THR^{487},HIS^{488},THR^{489},GLU^{492}, ARG^{493}	428

Site3 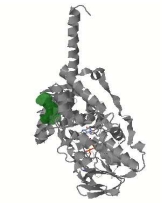	VAL^{101},LYS^{102},GLY^{103},ARG^{172},TYR^{175},LEU^{176},ASN^{179},GLU^{185},PRO^{186},ILE^{326},GLU^{327},ASP^{328}, GLU^{329},ASP^{330},SER^{334},LEU^{354},ALA^{355},ARG^{356},LYS^{357},ALA^{358},ARG^{360}	452
Site4 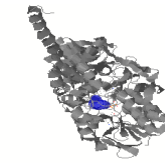	THR^{140},ASP^{141},ALA^{142},PRO^{143},TRP^{144},TRP^{193},TRP^{196},TYR^{197},LEU^{298},THR^{408},ALA^{409},TYR^{410},PHE^{411},MET^{416},GLY^{420},ILE^{423},ARG^{424},THR^{435},GLU^{436},THR^{437},ALA^{438},THR^{439},SER^{442},GLY^{443}	190
Site5 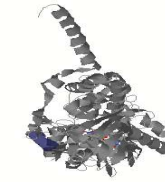	ASN^{75},ILE^{77},LEU^{78},ARG^{79},SER^{81},LYS^{82},ILE^{86},GLU^{87},THR^{88},PHE^{219},GLU^{475},PRO^{476},GLU^{477},SER^{478},LYS^{479},ASP^{480},VAL^{481}	185
Site6 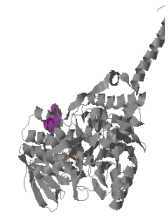	ARG^{76},ARG^{79},THR^{439},VAL^{449},GLU^{450},GLU^{453},ARG^{454},ARG^{457},ILE^{471},TRP^{472},VAL^{473},GLN^{474}, GLU^{475}	180
Site7 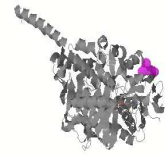	HIS^{246},THR^{278},ALA^{279},LYS^{280},ILE^{281},HIS^{282},PHE^{283},ARG^{284},GLU^{286},LEU^{287},ASN^{292},ILE^{295}, GLN^{296}	175
Site 8 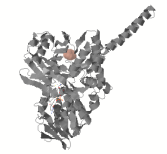	VAL^{93},LEU^{97},PHE^{108},ARG^{109},GLY^{110},ALA^{111},PHE^{208},SER^{209},VAL^{210},THR^{211},CYS^{323}	139
Site9 	ASN^{271},ILE^{273},PRO^{274},PRO^{275},THR^{278},ARG^{291},LEU^{294},ILE^{295},LEU^{298},ILE^{423},ARG^{424},PHE^{432},ALA^{433},GLY^{434},GLU^{436},THR^{437}	115

Site10 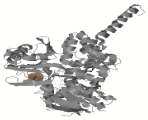	TYR^{62},VAL^{63},ASP^{64},ALA^{68},TYR^{89},LYS^{218},PHE^{219},VAL^{220},GLY^{221},GLY^{222},SER^{223}, LYS^{305},TYR^{309},ASP^{339},THR^{340},LYS^{341}	118

Ligand optimization and docking study

Discovery studio 3.1 was used for geometry optimization of the ligand structure. Three compounds (Baicalin [Chen X et al.,2007] , Curcumin [Mansouri Z et al.,2012] and Dronabinol [Pertwee, R.G.,2006]) were selected for docking study on the basis of earlier studies [Fig. 9] . Docking server was used to calculate molecular weight, molecular formula, molar weight and MMFF94 energy calculation of all retrieved compounds [Table 4]. Docking calculations are based on Est. Free Energy of Binding, Est. Inhibition Constant, vdW + H bond + desolv. Energy, Electrostatic Energy with MAO A and MAO B. Better interaction among compounds/drugs-protein is based on the docking intermolecular energy Specific inhibitors of MAOs were also used for the identification of interacting binding sites in MAOs model to evaluate the comparative binding sites for drugs/compounds.

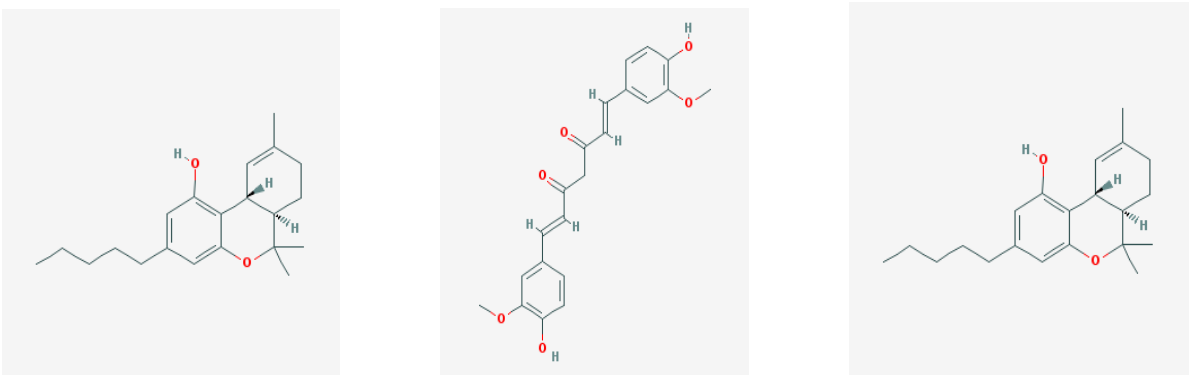

Figure 9: ***(a) Baicalin, (b) Curcumin, (c) Dronabinol***

Table 6: ***Chemical properties of compounds used for docking study***

CID	Structure	Compound Name	IUPAC name	Medicinal Plant Name	Molecular Weight (g/mol)	Molecular Formula	MMFF94 energy (kcal/mol)
16078	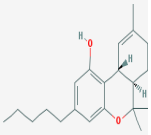	Baicalin	(6aR,10aR)-6,6,9-trimethyl-3-pentyl-6a,7,8,10a-tetrahydrobenzo[c]chromen-1-ol	*Scutellaria baicalensis*	314.4617	$C_{21}H_{30}O_2$	174.85432

969516	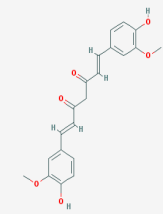	Curcumin	(1E,6E)-1,7-bis(4-hydroxy-3-methoxyphenyl)hepta-1,6-diene-3,5-dione	*Curcuma longa*	368.3799	$C_{21}H_{20}O_6$	65.92215
16078	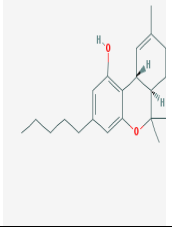	Dronabinol	(1R,10R)-9,9,13-trimethyl-5-pentyl-8-oxatricyclo [8.4.0.0^{2,7}]tetradeca-2,4,6,13-tetraen-3-olate	*Cannabis sativa*	314.461700	$C_{21}H_{30}O_2$	39.35010

Docking calculation of compounds with MAO A

MAO A interactions with Baicalin

Free energy of binding with Baicalin was -8.51 kcal/mol with 40% frequency and Est. Inhibition Constant, Ki was found to be 575.20 nM. VdW + Hbond + desolv Energy and Electrostatic Energy was -9.76 kcal/mol, -0.12 kcal/mol. Total Intermole. Energy and Interact. Surface was found to be -9.88 kcal/mol, 972.421 [Table 7 and Fig. 10a]. Active binding site residue of MAO A, PHE^{352},TYR^{407}, TYR^{444},MET^{445},ALA^{448} were involved in hydrophobic interactions and TYR^{69}, PHE^{352},TYR^{407},TYR^{444} were in cation Pi interactions. TYR^{444} was responsible for H-bonding while TYR^{407} in PI-PI interaction. Polar interactions were because of ASN^{181}, GLN215, TYR407 and TYR444 [Table 9 and Fig.11].

MAO A interactions with curcumin

Free energy of binding with curcumin was -7.95 kcal/mol with 60% frequency and Est. Inhibition Constant, Ki was found to be 1.48 uM. vdW + Hbond + desolv Energy and Electrostatic Energy were -10.44 kcal/mol and -0.14 kcal/mol. Total Intermole. Energy and Interact. Surface was found to be-10.58 kcal/mol, 1009.377 respectively [Table 5 and Fig. 10b]. Active binding site residue of MAO A, ILE^{23},TYR^{69}, ILE^{180},ILE^{335},PHE^{352}, TYR^{407} were involved in hydrophobic interactions and PHE^{352}, TYR^{407} in PI-PI interaction. ARG^{51}, ASN^{181}, GLN^{215}, LYS^{305} were responsible for polar interactions [Table 7 and Fig.11].

MAO A interactions with Dronabinol

Free energy of binding with Dronabinol was -10.28 kcal/mol kcal/mol with 50% frequency and Est. Inhibition Constant, Ki was found to be 29.22 nM. VdW + Hbond + desolv Energy and Electrostatic Energy was -11.62 kcal/mol, -0.06 kcal/mol. Total Intermole. Energy and Interact. Surface was found to be -11.68 kcal/mol, 938.968 respectively [Table 7 and Fig. 10c]. ILE^{23}, PHE352, TYR407, TYR444, MET445, ALA448 were involved in hydrophobic interactions, TYR407 was in cation Pi interactions and ARG^{51} in Polar interactions [Table 9 and Fig.11].

Table 7: ***Docking calculation of compounds with MAO A***

Compound Name	Est. Free Energy of Binding	Est. Inhibition Constant, Ki	vdW + Hbond + desolv Energy	Electrostatic Energy	Total Intermole. Energy	Frequency	Interact. Surface
Baicalin	-8.51 kcal/mol	575.20 nM	-9.76 kcal/mol	-0.12 kcal/mol	-9.88 kcal/mol	40%	972.421
curcumin	-7.95	1.48 uM	-10.44	-0.14	-10.58	60%	1009.377

	kcal/mol		kcal/mol	kcal/mol	kcal/mol		
Dronabinol	-10.28 kcal/mol	29.22 nM	-11.62 kcal/mol	-0.06 kcal/mol	-11.68 kcal/mol	50%	938.968

Docking calculation of compounds with MAO B

MAO B interactions with Baicalin

Free energy of binding with Baicalin was -9.23 kcal/mol with 60% frequency and Est. Inhibition Constant, Ki was found to be 170.64 nM and VdW + Hbond + desolv Energy and Electrostatic Energy was -11.08 kcal/mol and -0.06 kcal/mol .Total Intermole. Energy and Interact. Surface was found to be -11.14 kcal/mol and 664.692 [Table 6 and Fig. 12a]. TYR^{326}, TYR398, TYR^{435} were involved in hydrophobic interactions, TYR^{60}, PHE^{343}, TYR^{398}, TYR^{435} were in cation Pi interactions and GLN^{206}, TYR^{435} were in polar interactions. Only TYR^{398} was responsible for PI-PI interaction [Table 7and Fig.13a].

MAO B interactions with Curcumin

Free energy of binding with Curcumin was -7.79 kcal/mol with 40% frequency and Est. Inhibition Constant, Ki was found to be 1.94 uM. VdW + Hbond + desolv Energy and Electrostatic Energy were -10.61 kcal/mol and -0.03 kcal/mol. Total Intermole. Energy and Interact. Surface was found to be -10.64 kcal/mol, 685.358 respectively [Table 6 and Fig. 12b]. TYR^{326}, PHE343, TYR^{398}, MET^{436} were involved in hydrophobic interactions, PHE^{343}, TYR^{398} and ARG^{42}, GLN^{206} were in polar interactions [Table 7and Fig.13b].

MAO B interactions with Dronabinol

Free energy of binding with Dronabinol was -9.55 kcal/mol with 80% frequency and Est. Inhibition Constant, Ki was found to be 100.45 nM. VdW + Hbond + desolv Energy and Electrostatic Energy was -10.97 kcal/mol, -0.00 kcal/mol. Total Intermole. Energy and Interact. Surface was found to be -10.97 kcal/mol, 595.882 respectively [Table 6 and Fig. 12c]. LEU^{171}, PHE343, TRP^{388}, CYS397, TYR^{398}, TYR^{435} were involved in hydrophobic interactions, TYR^{60}, TYR^{435} in PI-PI interaction and TYR^{60} was in cation Pi interactions. SER^{59}, LYS^{296} were responsible for polar interactions [Table 7and Fig.13c].

Table 8: ***Docking calculation of compounds with MAO B***

Compound Name	Est. Free Energy of Binding	Est. Inhibition Constant, Ki	vdW + Hbond + desolv Energy	Electrostatic Energy	Total Intermole. Energy	Frequency	Interact. Surface
Baicalin	-9.23 kcal/mol	170.64 nM	-11.08 kcal/mol	-0.06 kcal/mol	-11.14 kcal/mol	60%	664.692
curcumin	-7.79 kcal/mol	1.94 uM	-10.61 kcal/mol	-0.03 kcal/mol	-10.64 kcal/mol	40%	685.358
Dronabinol	-9.55 kcal/mol	100.45 nM	-10.97 kcal/mol	-0.00 kcal/mol	-10.97 kcal/mol	80%	595.882

Table 9: ***MAO A & B residues participated during interaction at H-bond, polar, hydrophobic, pi-pi and cation-pi level.***

	INTERACTION	H-BOND	POLAR	HYDROPHOBIC	PI-PI	CATION-PI
MAO A	**Baicalin**	TYR^{444}	ASN^{181},GLN^{215}, TYR^{407}, TYR^{444}	PHE^{352},TYR^{407},TYR^{444}, MET^{445},ALA^{448}	TYR^{407}	TYR^{69}, PHE^{352}, TYR^{407},TYR^{444}
	curcumin		ARG^{51},ASN^{181}, GLN^{215}, LYS^{305}	ILE^{23},TYR^{69},ILE^{180}, ILE^{335},PHE^{352}, TYR^{407}	PHE^{352}, TYR^{407}	
	Dronabinol		ARG^{51}	ILE^{23},PHE^{352},TYR^{407}, TYR^{444},MET^{445}, ALA^{448}		TYR^{407}
MAO	**Baicalin**		GLN^{206}, TYR^{435}	TYR^{326},TYR^{398}, TYR^{435}	TYR^{398}	TYR^{60}, PHE^{343},

B					TYR^{398}, TYR^{435}
	curcumin	ARG^{42}, GLN^{206}	TYR^{326},PHE^{343}, MET^{436}	TYR^{398},	PHE^{343}, TYR^{398}
	Dronabinol	SER^{59}, LYS^{296}	LEU^{171},PHE^{343},TRP^{388}, CYS^{397}, TYR^{398}, TYR^{435}		TYR^{60}, TYR^{435} TYR^{60}

Docking result of MAO A

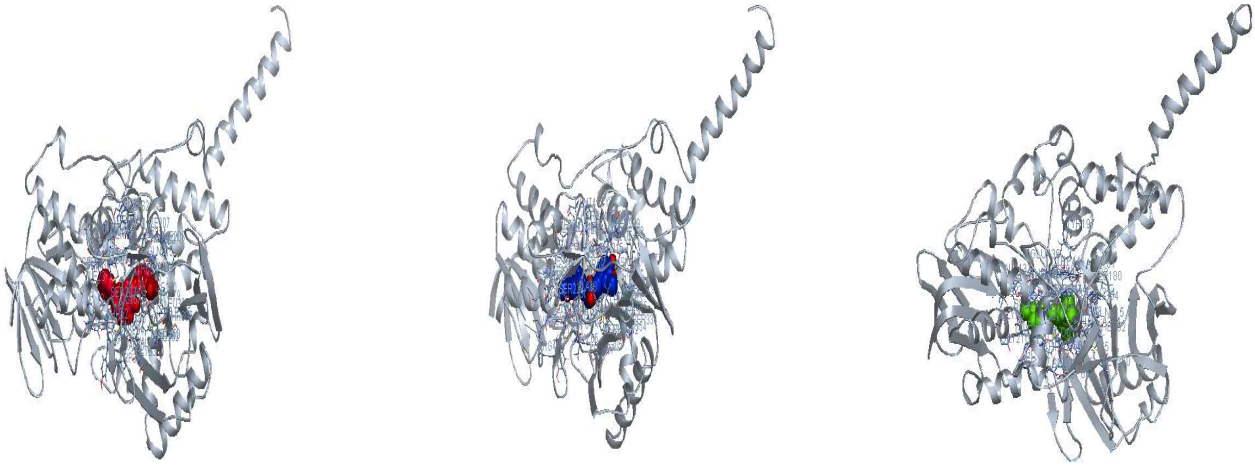

Figure 10 : ***(a) Docking of MAO A with Baicalin (b) Curcumin (c) Dronabinol***

Interacting residues of MAO A

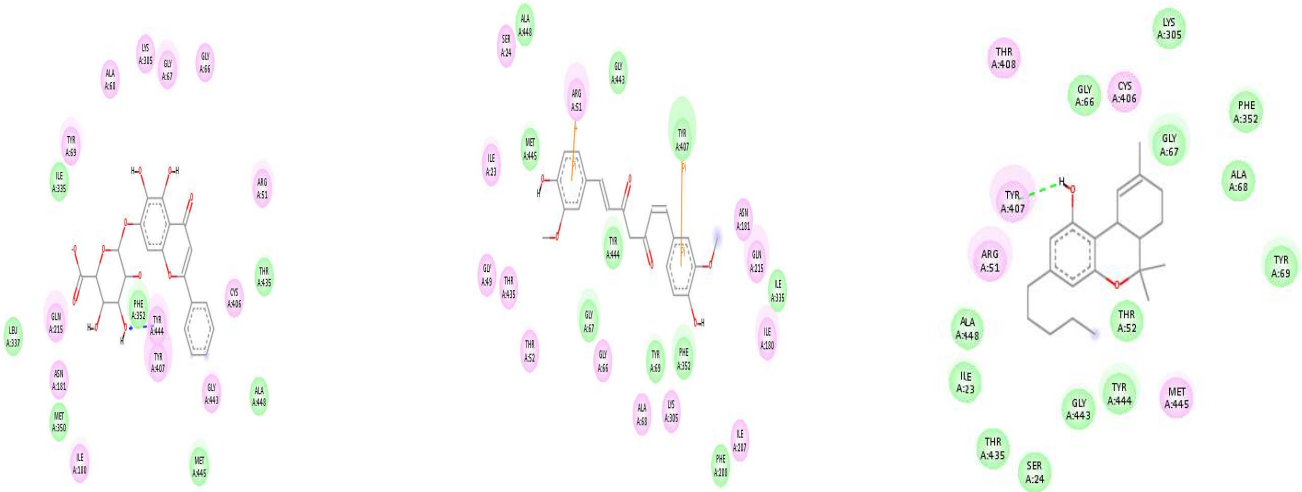

Figure 11(a) ***Interactions of residues with Baicalin (b) Curcumin (c) Dronabinol***

Docking of MAO B

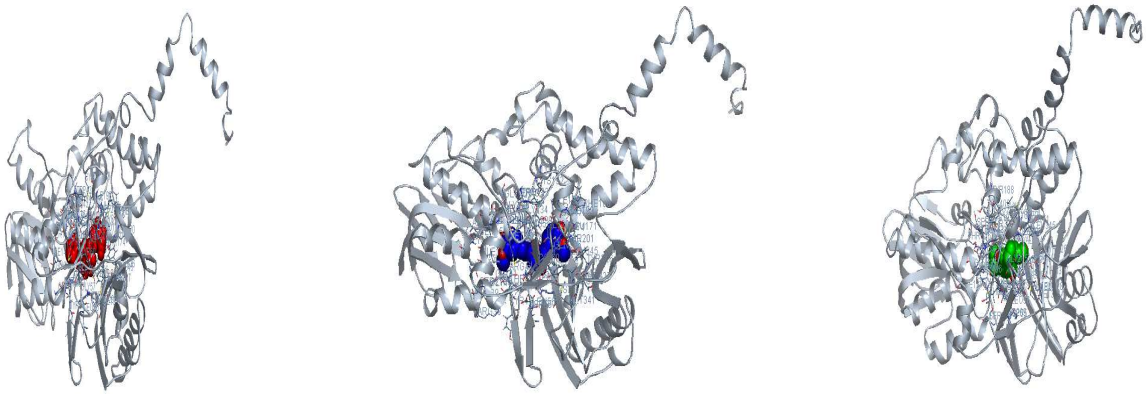

Figure 12: (a) ***Docking of MAO B with Baicalin (b) Curcumin (c) Dronabinol***

Interacting residues of MAO B

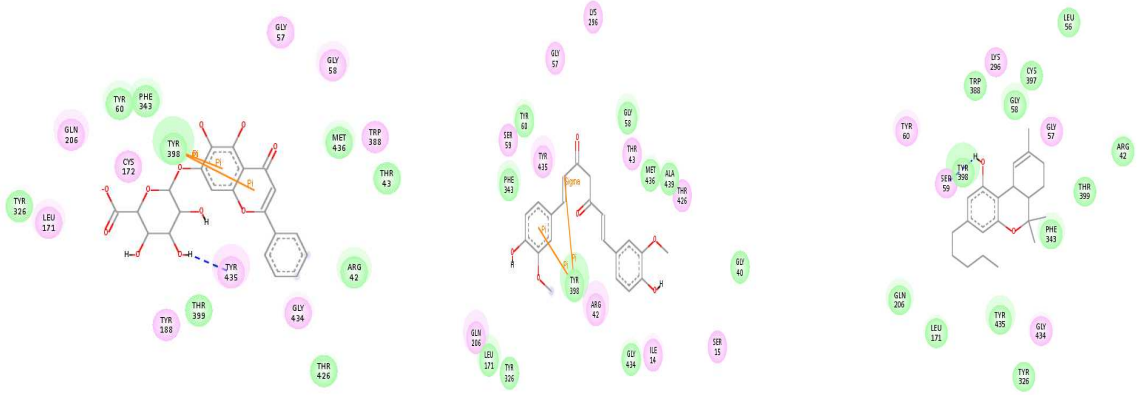

Figure 13(a) ***Interactions of MAO B residues with (a) Baicalin (b) Curcumin (c) Dronabinol***

Binding site of MAOs template with reported Inhibitor and MAOs model with docked compounds

Binding site residues of MAO A and MAO B interacting Baicalin, Curcumin and Dronabinol was found to be the same as the template residues involved in binding with earlier used inhibitor [Table 8]. Interacting residues of MAO A template with its inhibitor were ILE^{19},GLY^{20},GLY^{21},GLY^{22},ILE^{23},SER^{24},LEU^{42},GLU^{43},ALA^{44},ARG^{45},GLY^{49},GLY^{50},ARG^{51},GLY^{66},GLY^{67},ALA^{68},TYR^{69},TRP^{116},PRO^{118},TYR^{121},ILE^{180},ASN^{181},PHE^{208},GLN^{215},PRO^{243},ALA^{272},ILE^{273},LEU^{277},ILE^{335},LEU^{337},PHE^{352},TRP^{397},TYR^{402},CYS^{406},TYR^{407},GLY^{434},THR^{435},GLY^{443},TYR^{444},MET^{445},ALA^{448},THR489,TRP^{491},GLU^{492},THR^{509}. Interacting residues in case of Baicalin were ARG^{51}, GLY^{66},GLY^{67},ALA^{68},TYR^{69}, ILE^{180}, GLN^{215}, LYS^{305},LEU^{337}, PHE^{352}, CYS^{406},TYR^{407}, THR^{435}, TYR^{444},MET^{445} and in case of Curcumin were ILE^{23},GLY^{49},ARG^{51},THR^{52},GLY^{67},ALA^{68},TYR^{69},ILE^{180},ASN^{18},GLN^{215}, LYS^{305}, PHE^{352}, TYR^{407},THR^{435},GLY^{443},TYR^{444}. While ILE^{23}, SER^{24}, ARG^{51}, GLY^{66}, GLY^{67}, ALA^{68}, TYR^{69}, LYS^{305}, PHE^{352}, CYS^{406}, TYR^{407}, TYR^{444}, MET^{445} residues were interacting residues in case of Dronabinol [Table 10].

Interacting residues of MAO B template with its inhibitor were VAL^{10}, GLY^{11}, GLY^{12}, GLY^{13}, ILE^{14}, SER^{15}, GLU^{34}, ARG^{36}, GLY^{41}, ARG42, GLY^{57}, GLY^{58}, SER^{59}, TYR^{60}, LEU^{171}, CYS^{172}, GLN ^{206}, VAL^{235}, ILE^{264}, TYR^{393}, CYS^{397}, TYR^{398},

GLY^{425}, THR^{426}, GLY^{434}, TYR^{435}, MET^{436} and ALA439. Interacting residues in case of Baicalin were ARG^{42}, GLY^{57}, GLY^{58}, TYR^{60,} LEU^{171}, CYS^{172}, TYR^{188}, GLN ^{206}, TYR^{326}, PHE^{343}, TRP^{388}, TYR^{398}, THR^{426}, GLY^{434} and TYR435 and in case of Curcumin were ILE^{14}, GLY^{40}, ARG^{42}, THR^{43}, GLY^{57}, GLY^{58}, TYR^{60}, LYS^{296}, TYR^{326}, PHE^{343}, TYR^{398}, THR^{426}, GLY^{434}, TYR^{435}, MET^{436} and ALA^{439}. GLY^{57}, GLY^{58} , SER^{59}, TYR^{60}, LEU^{171}, GLN ^{206}, LYS^{296}, PHE^{343}, TRP^{388}, CYS^{397}, TYR^{398}, GLY^{434}, TYR^{435} residues were interacting residues in case of Dronabinol [Table 11].

Table 10: ***MAOA interacting residues with known inhibitor and selected compounds***

Compound	Interacting residues
Known inhibitory Active site	ILE^{19,}GLY^{20},GLY^{21},GLY^{22,}ILE^{23},SER^{24},LEU^{42},GLU^{43},ALA^{44},ARG^{45},GLY^{49},GLY^{50},ARG^{51},GLY^{66},GLY^{67}, ALA^{68},TYR^{69},TRP^{116},PRO^{118},TYR^{121},ILE^{180},ASN^{181},PHE^{208},GLN^{215},PRO^{243},ALA^{272},ILE^{273},LEU^{277},ILE^{335}, LEU^{337},PHE^{352},TRP^{397},TYR^{402},CYS^{406},TYR^{407},GLY^{434},THR^{435},GLY^{443},TYR^{444},MET^{445},ALA^{448},THR489, TRP^{491},GLU^{492},THR^{509}
Baicalin	ARG^{51}, GLY^{66},GLY^{67},ALA^{68},TYR^{69}, ILE^{180}, GLN^{215}, LYS^{305},LEU^{337}, PHE^{352}, CYS^{406},TYR^{407}, THR^{435}, TYR^{444},MET^{445}
curcumin	ILE^{23},GLY^{49},ARG^{51},THR^{52},GLY^{67},ALA^{68},TYR^{69},ILE^{180},ASN^{18}, GLN^{215}, LYS^{305}, PHE^{352}, TYR^{407}, THR^{435}, GLY^{443},TYR^{444}
Dronabinol	ILE^{23},SER^{24}, ARG^{51},GLY^{66},GLY^{67},ALA^{68},TYR^{69}, LYS^{305},PHE^{352},CYS^{406},TYR^{407},TYR^{444},MET^{445},

Table 11: ***MAO B interacting residues with known inhibitor and selected compounds***

Compound	Interacting residues
Known inhibitory Active site	VAL^{10}, GLY^{11}, GLY^{12}, GLY^{13}, ILE^{14}, SER^{15}, GLU^{34}, ARG^{36}, GLY^{41},ARG^{42}, GLY^{57}, GLY^{58} , SER^{59}, TYR^{60}, LEU^{171}, CYS^{172}, GLN ^{206}, VAL^{235}, ILE^{264}, TYR^{393}, CYS^{397}, TYR^{398}, GLY^{425}, THR^{426}, GLY^{434}, TYR^{435}, MET^{436}, ALA^{439}
Baicalin	ARG^{42}, GLY^{57}, GLY^{58} , TYR^{60} , LEU^{171}, CYS^{172}, TYR^{188}, GLN ^{206}, TYR^{326}, PHE^{343}, TRP^{388}, TYR^{398}, THR^{426}, GLY^{434}, TYR^{435}
curcumin	ILE^{14}, GLY^{40}, ARG^{42}, THR^{43}, GLY^{57}, GLY^{58} , TYR^{60}, LYS^{296}, TYR^{326}, PHE^{343}, TYR^{398}, THR^{426}, GLY^{434}, TYR^{435}, MET^{436}, ALA^{439}
Dronabinol	GLY^{57}, GLY^{58} , SER^{59}, TYR^{60}, LEU^{171}, GLN ^{206}, LYS^{296}, PHE^{343}, TRP^{388}, CYS^{397}, TYR^{398}, GLY^{434}, TYR^{435}

DISCUSSION

By this *Insilico* investigation, we have successfully hunted 14 unique hits based on functional domain sequence using Interproscan server and optimized 14 full length genes of amine oxidase family. These isoforms belong to six amine oxidase gene family: Polyamine Oxidase (PAO), Monoamine Oxidase (MAO), L-amino acid oxidase (LAO), Protoporphyrinogen Oxidase (PPOX), Lysine Specific Histone Demethylase (LSHD) and Spermine Oxidase (SOX) genes and catalyze different functions like oxidative deamination of neuroactive and vasoactive amines, apoptosis and cell proliferation, metabolism of some amino acids, control developmental and transcriptional programs, heme biosynthesis and deficiency causes genetic disease variegate porphyria, potentially mutagenic DNA damage and inflammation-induced carcinogenesis respectively. Monoamine oxidase enzyme exists in two forms A and B and play very important role in Parkinson's disease and inhibitors of type B monoamine oxidase are the most promising neuroprotective agents to date [Naoi M et al., 2010]. So MAO isoforms were selected for the *insilico* study to find the interaction and effect of herbal compounds on MAO proteins. Phylogenetic study revealed that PPOX was different from others, MAO and LAO in one cluster as share more homology while LSHD, SMOX and PAO in another cluster.

Chromosomal localization of isoforms was determined and found that MAO isoforms were located on X chromosome. ProtParam results

showed that an isoelectric point was 7.94 and 7.20 for MAO A and MAO B which indicates positively charged proteins and negative GRAVY index of -0.279 and -0.236 score indicate that these proteins are hydrophilic and soluble in nature and we have also found that MAO A composition was found to be Glycine rich while MAO B was Leucine rich . Templates showed 99% sequence identity for both MAO A and MAO B. 3D structure of MAO A and MAO B were generated by using Swiss Model Server. Z score for MAO A and MAO B was 0.382, 0.614, suggesting that input structure is within the range of scores typically found for native proteins of similar size. RAMPAGE displayed 97.8% of residues in the most favoured regions, 2.2% residues in additionally allowed and 0.0% disallowed regions for MAO A model and in case of MAO B model 96.5% residues in the most favoured regions, 3.5% residues in additionally allowed and 0.0% residues in disallowed regions, showing that stereo chemical quality of protein structure is good. Result of Errat showed 97.426% accurate structure for MAO A and 80.354% for MAO B. The final protein structures are available with PMDB ID: PM0077964 and PM0077935. Among the ten binding sites obtained from Q-SiteFinder for MAO A and MAO B, site 1 was highly conserved within the active site of the template. Active site prediction is useful to determine potential sites for ligand binding in molecular docking. Three compounds (Baicalin, Curcumin and Dronabinol) which are extracted from different medicinal plants were selected for molecular docking study at *In-silico* level.

Docking study revealed that all three compounds are interacting at the reported active binding site and binding atomic coordination were compared with the template complex coordination and found that docked drug coordination was similar with the known coordination. Inhibition Constant, Ki of Baicalin, Curcumin and Dronabinol for MAO A was found to be 575.20 nM, 1.48 uM and 29.22 nM respectively while 170.64 nM, 1.94 uM and 100.45 nM for MAO B, suggesting that all the selected compounds are effective as MAO inhibitors. Amino acid residues MAO A and MAO B involved in interaction with Baicalin, Curcumin and Dronabinol were found to be the same as the template residues involved in binding with earlier used inhibitors. This indicates that we can efficiently determine active site coordinate with target and template active site residue to investigate the effect of inhibitors on the functional active site of enzymes. Investigation of active binding sites within MAO proteins and comparison with the known active binding site gives a better idea for a valuable drug target site and drug interaction with highest affinity. In this result the most effective compound was found to be Dronabinol as showing minimum Inhibition Constant, Ki and lowest free energy of binding with maximum interacting surface area for both models.

REFERENCES

1. Altschul SF, Gish W, Miller W, Myers EW, Lipman DJ. Basic local alignment search tool. J Mol Biol. 1990; 215(3):403-10. PMID: 2231712.
2. Arnold K, Bordoli L, Kopp J, Schwede T. The SWISS-MODEL workspace: a web-based environment for protein structure homology modelling. Bioinformatics. 2006; 22(2):195-201. PMID: 16301204.
3. Bikadi Z, Hazai E. Application of the PM6 semi-empirical method to modeling proteins enhances docking accuracy of AutoDock. J Cheminform. 2009; 1:15. PMID: 20150996;
4. Bikadi Z, Demko L, Hazai E. Functional and structural characterization of a protein based on analysis of its hydrogen bonding network by hydrogen bonding plot. Arch Biochem Biophys. 2007; 461(2):225-34. PMID: 17391641.
5. Chen X, Zhang N, Zou HY. Protective effect of baicalin on mouse with Parkinson's disease induced by MPTP. Zhongguo Zhong Xi Yi Jie He Za Zhi. 2007 ;(11):1010-2. PMID: 18173149.
6. Kleinman A, Tieppo CA, Florez GM, Felicio LF, Nasello AG. Rapidly induced

dopaminergic supersensitivity: D1/D2 receptor participation and its prevention by an MAO-inhibitor. Pharmacol Biochem Behav. 2006; 85(3):592-600. PMID: 17157367.
7. Laurie AT, Jackson RM. Q-SiteFinder: an energy-based method for the prediction of protein-ligand binding sites. Bioinformatics. 2005; 21(9):1908-16. PMID: 15701681.
8. Mansouri Z, Sabetkasaei M, Moradi F, Masoudnia F, Ataie A. Curcumin has Neuroprotection Effect on Homocysteine Rat Model of Parkinson. J Mol Neurosci. 2012 Mar 15. PMID: 22418789.
9. McDonald IK, Thornton JM. Satisfying hydrogen bonding potential in proteins. J Mol Biol. 1994 ;238(5):777-93. PMID: 8182748.
10. Naoi M, Maruyama W. Monoamine oxidase inhibitors as neuroprotective agents in age-dependent neurodegenerative disorders. Curr Pharm Des. 2010; (25):2799-817. Review. PMID: 20698822.
11. Pertwee, R. G. "The pharmacology of cannabinoid receptors and their ligands: An overview". International Journal of Obesity 2006; **30**: S13–S18.. PMID 16570099.
12. Schwede T, Kopp J, Guex N, Peitsch MC. SWISS-MODEL: An automated protein homology-modeling server. Nucleic Acids Res. 2003; 31(13):3381-5. PMID: 12824332;
13. Shih JC, Chen K, Ridd MJ. Role of MAO A and B in neurotransmitter metabolism and behavior. Pol J Pharmacol. 1999;51(1):25-9. Review. PMID: 10389141.
14. Thompson JD, Gibson TJ, Higgins DG. Multiple sequence alignment using ClustalW and ClustalX. Curr Protoc Bioinformatics. 2002; Aug;Chapter 2:Unit 2.3. PMID: 18792934.
15. Yang Z, Lasker K, Schneidman-Duhovny D, Webb B, Huang CC, Pettersen EF, Goddard TD, Meng EC, Sali A, Ferrin TE. UCSF Chimera, MODELLER, and IMP: An integrated modeling system. J Struct Biol. 2011; PMID: 21963794.